JB Journals.ASM.org

Role of RNA Secondary Structure and Processing in Stability of the *nifH1* Transcript in the Cyanobacterium *Anabaena variabilis*

Brenda S. Pratte, Justin Ungerer, Teresa Thiel

University of Missouri—St. Louis, Department of Biology, St. Louis, Missouri, USA

ABSTRACT

In the cyanobacterium *Anabaena variabilis* ATCC 29413, aerobic nitrogen fixation occurs in micro-oxic cells called heterocysts. Synthesis of nitrogenase in heterocysts requires expression of the large *nif1* gene cluster, which is primarily under the control of the promoter for the first gene, *nifB1*. Strong expression of *nifH1* requires the *nifB1* promoter but is also controlled by RNA processing, which leads to increased *nifH1* transcript stability. The processing of the primary *nifH1* transcript occurs at the base of a predicted stem-loop structure that is conserved in many heterocystous cyanobacteria. Mutations that changed the predicted secondary structure or changed the sequence of the stem-loop had detrimental effects on the amount of *nifH1* transcript, with mutations that altered or destabilized the structure having the strongest effect. Just upstream from the transcriptional processing site for *nifH1* was the promoter for a small antisense RNA, *sava4870.1*. This RNA was more strongly expressed in cells grown in the presence of fixed nitrogen and was downregulated in cells 24 h after nitrogen step down. A mutant strain lacking the promoter for *sava4870.1* showed delayed nitrogen fixation; however, that phenotype might have resulted from an effect of the mutation on the processing of the *nifH1* transcript. The *nifH1* transcript was the most abundant and most stable *nif1* transcript, while *nifD1* and *nifK1*, just downstream of *nifH1*, were present in much smaller amounts and were less stable. The *nifD1* and *nifK1* transcripts were also processed at sites just upstream of *nifD1* and *nifK1*.

IMPORTANCE

In the filamentous cyanobacterium *Anabaena variabilis*, the *nif1* cluster, encoding the primary Mo nitrogenase, functions under aerobic growth conditions in specialized cells called heterocysts that develop in response to starvation for fixed nitrogen. The large cluster comprising more than a dozen *nif1* genes is transcribed primarily from the promoter for the first gene, *nifB1*; however, this does not explain the large amount of transcript for the structural genes *nifH1*, *nifD1*, and *nifK1*, which are also under the control of the distant *nifB1* promoter. Here, we demonstrate the importance of a predicted stem-loop structure upstream of *nifH1* that controls the abundance of *nifH1* transcript through transcript processing and stabilization and show that *nifD1* and *nifK1* transcripts are also controlled by transcript processing.

Anabaena variabilis is a filamentous cyanobacterium that fixes nitrogen under oxic growth conditions in cells called heterocysts. Heterocysts, which are specialized micro-oxic cells that develop in a semiregular pattern in the filament in response to nitrogen stress, fix atmospheric dinitrogen to ammonium using the enzyme nitrogenase (1–3). The micro-oxic conditions of the heterocyst result from the glycolipid layer that may restrict oxygen diffusion into the cell, the absence of oxygen-evolving photosystem II, and increased respiration, all of which serve to protect nitrogenase from oxygen (4–6). While all heterocyst-forming cyanobacteria make a Mo nitrogenase that functions in heterocysts, *A. variabilis* is unusual because it has three nitrogenases, two Mo nitrogenases and one V nitrogenase (reviewed in reference 7). The primary nitrogenase, which is expressed in heterocysts in cultures growing in air in an environment with adequate molybdate, is a Mo nitrogenase encoded by the *nif1* genes (8, 9). The Nif1 nitrogenase is expressed late in heterocyst differentiation, after the cell becomes micro-oxic (10). Under similar growth conditions, but in an environment deficient in molybdate but with adequate vanadate, heterocysts make an alternative, V nitrogenase, encoded by the *vnf* genes (8, 11). The V nitrogenase is completely repressed in the presence of molybdate. The second Mo nitrogenase, encoded by the *nif2* genes, is made only in anoxic vegetative cells in an environment with adequate molybdate (12). Synthesis of all three nitrogenases is repressed in cells grown with a source of fixed nitrogen (+N).

Nitrogenase synthesis requires the products of at least a dozen genes, most of which are encoded by conserved genes that are found in large *nif* clusters in all nitrogen-fixing bacteria. Dimers of NifD (α-subunit) and NifK (β-subunit) make up the heterotetrameric dinitrogenase with two M clusters (comprising $MoFe_7S_9C$-homocitrate) (13–16). NifH is dinitrogenase reductase with an $[Fe_4\text{-}S_4]$ cofactor, which transfers electrons to dinitrogenase (17). NifS transfers sulfur from cysteine to NifU (18), which acts as a scaffolding protein for [Fe-S] cluster assembly (15, 19). The [Fe-S] clusters are transferred to NifB to make NifB-co, an $[Fe_6\text{-}S_9]$ cluster that serves as the precursor to the M cluster (20, 21). NifE and

Received 29 December 2014 **Accepted** 30 January 2015

Accepted manuscript posted online 9 February 2015

Citation Pratte BS, Ungerer J, Thiel T. 2015. Role of RNA secondary structure and processing in stability of the *nifH1* transcript in the cyanobacterium *Anabaena variabilis*. J Bacteriol 197:1408–1422. doi:10.1128/JB.02609-14.

Editor: J. P. Armitage

Address correspondence to Teresa Thiel, thiel@umsl.edu.

Supplemental material for this article may be found at http://dx.doi.org/10.1128/JB.02609-14.

doi:10.1128/JB.02609-14

NifN, which are homologs of NifD and NifK, form a similar heterotetrameric complex and serve as a scaffold for M cluster assembly prior to its transfer to aponitrogenase (15, 22). NifW is involved in the processing of homocitrate (23), while NifX may function as a reservoir of FeMo cofactor (24). NifV makes homocitrate, a component of FeMo cofactor (15), while NifZ is involved in P cluster assembly (25, 26). Missing in cyanobacteria are the genes for NifQ, the Mo donor to FeMo cofactor (27); NifM, which stabilizes NifH (28, 29); and NafY, which stabilizes the open conformation of apo-MoFe protein prior to the insertion of the M cluster (30, 31). In *A. variabilis*, the organizations of the *nif* clusters for *nif1* and *nif2* are similar, but the *nif2* cluster lacks the 11-kb excision element that interrupts *nifD1* in the *nif1* cluster and the *nifEN* genes are fused into a single open reading frame (ORF) in the *nif2* cluster (7). The Mo-repressed *vnf* genes in *A. variabilis* are not tightly clustered but are found within a region of about 40 kb, which includes many uncharacterized genes (7). In addition to the structural genes, *vnfH*, *vnfDG*, and *vnfK*, there are the genes for scaffolding proteins, *vnfEN*, and the vanadate transport genes, *vupABC* (32, 33).

In the *Proteobacteria*, *nif* genes are under the control of the NtrBC nitrogen-regulatory system, which controls synthesis of the regulatory proteins NifA and NifL (34). Activation of *nif* genes in the absence of oxygen and fixed nitrogen (−N) requires NifA or VnfA, as well as the alternative δ^{54} RNA polymerase (34). In cyanobacteria, there are no homologs of NtrBC, NifA, NifL, or VnfA. While no sigma factor specifically associated with nitrogen regulation, like the δ^{54} factor in *Proteobacteria*, has been identified in cyanobacteria, the sigma factor encoded by *sigE* is important, but not essential, for expression of the *nif* genes in *Anabaena* sp. strain PCC 7120 (35).

Regulation of nitrogenase expression in cyanobacteria is not well understood. The global regulator NtcA affects the expression of genes that respond to nitrogen availability in all cyanobacteria; however, in heterocyst-forming cyanobacteria, it plays a key role in sensing nitrogen starvation and initiating the complex process of heterocyst differentiation (1, 2). NtcA has been reported to bind weakly to a region upstream of *nifH* in *Anabaena* sp. PCC 7120, and a putative noncanonical NtcA binding site was identified (36, 37). However, a chromatin immunoprecipitation sequencing (ChIP-seq) analysis of RNA from *Anabaena* sp. PCC 7120 showed that NtcA binds to a site inside *nifH* in *Anabaena* sp. PCC 7120 (38). We were unable to detect binding of NtcA to the intergenic *nifU1-nifH1* region of *A. variabilis*, and mutations in the putative NtcA binding site in the strain did not affect nitrogenase expression (39). This is consistent with the fact that there is no promoter in the *nifUH1* intergenic region.

Within the large *nif* cluster of *Anabaena* sp. PCC 7120, putative transcription start sites (tss) have been identified for *nifB*, *nifH*, *hesA*, and *fdxH* (36, 39–45). Transcription of the *nif1* gene cluster of *A. variabilis* depends primarily on the promoter for the first gene in the cluster, *nifB1* (39). The apparent transcription start sites for *nifB1* and *nifH1* in *A. variabilis* are identical to those mapped in *Anabaena* sp. PCC 7120, and there are weak, heterocyst-specific promoters within the coding regions of *nifU1* and *nifE1* (7, 39, 46). However, we found no evidence for a promoter in the 300-bp *nifU1-nifH1* intergenic region driving expression of *nifH1* (39). In contrast, we were able to verify primary transcription start sites upstream of *nifB1* and *hesA1* that matched the published sequence (7, 39, 46). Further, we demonstrated that the 5′ ends of *nifH1* and *fdxH1* in the *nif1* cluster, as well as the V-nitrogenase genes, *vnfH* and *vnfDG*, have processed RNA ends, not primary transcript ends (39, 46, 47). In a mutant strain that lacks *xisA*, the gene that makes the excisase that removes the 11-kb element from *nifD1*, the *nifB1* promoter can no longer drive expression of the genes downstream from the excision element, resulting in little or no expression of those genes (46). Even *hesA1*, which has its own promoter, is not expressed as well in the *xisA* mutant as in the wild-type (WT) strain, which suggests that the *nifB1* promoter controls the expression of a gene that is 14 kb away.

The *nifH* gene is highly expressed because it is required in large amounts both for assembly of nitrogenase and for the function of the enzyme (16). In *A. variabilis*, the *nifH1* transcript is much more abundant than the other *nif1* transcripts, even though *nifH1* lacks its own promoter, because the transcript is very stable (39, 46). The 5′ end of the processed transcript is at the base of a predicted stem-loop structure that may be responsible for the stability of the transcript (39, 46). We have examined the region between *nifU1* and *nifH1*, including the predicted stem-loop structure located 123 bp upstream of *nifH1* and an antisense RNA whose transcript begins near the predicted stem-loop structure, to determine the role of the region in the transcript abundance of *nifH1*.

MATERIALS AND METHODS

Strains and growth conditions. *A. variabilis* strain FD, a derivative of *A. variabilis* ATCC 29413, can grow at 40°C. FD and derivatives of the strain were maintained on agar-solidified Allen and Arnon (AA) medium (48) supplemented, when appropriate, with 5 mM NH_4Cl, 10 mM *N*-tris(hydroxymethyl)methyl-2-aminoethanesulfonic acid (TES), pH 7.2, 40 μg ml^{-1} neomycin sulfate, 3 μg ml^{-1} each of spectinomycin and streptomycin, or 5 μg ml^{-1} erythromycin. Strains were grown photoautotrophically in liquid cultures in an 8-fold dilution of AA medium (AA/8) or in AA/8 supplemented with 5 mM NH_4Cl and 10 mM TES, pH 7.2, at 30°C, with illumination at 100 to 120 microeinsteins m^{-2} s^{-1}. Antibiotics, when used, included neomycin (5 μg ml^{-1}), erythromycin (1 μg ml^{-1}), and spectinomycin (0.5 μg ml^{-1}). Growth, as the growth constant μ, was measured in triplicate cultures as the optical density at 720 nm (OD_{720}) in very dilute cultures (to prevent self-shading) that grew exponentially over three cell divisions, as described previously (46).

Construction of strains. The construction of all plasmids is briefly described in Table 1, and all the primers used in the construction of strains are shown in Table 2. Strains BP703, BP706, and BP712 were constructed by making two PCR products that included the mutations of interest flanked by wild-type regions for recombination, allowing us to replace the wild-type region in the chromosome with the mutations in the PCR products. Mutations that destroyed the predicted stem-loop structure in the *nifUH1* intergenic region (BP706) were constructed using primer sets nifHLoop1-L/nifHLoop1-R and nifHMutLoop2-L/nifHLoop2-R. Mutations that restored a stem-loop with different nucleotides (BP703) were constructed using primer sets nifHLoop1-L/nifHLoop1-R and nifHResLoop2-L/nifHLoop2-R. Mutation in the promoter for the antisense gene *sava4870.1* was constructed using primer sets antiloopmut-1/antiloopmut-2 and antiloopmut-3/antiloopmut-4. The pairs of PCR products were triply ligated into the PstI/KpnI sites of pUC18 to create pBP701, pBP700, and pBP711, respectively. A 6-kb SacI fragment of pRL2948a, containing the *mob* site for mobilization, *sacB* for sucrose selection of double recombinants, and an erythromycin resistance (Em^r) gene (49), was inserted into the SacI site in pBP700, pBP701, and pBP711 to create pBP703, pBP706, and pBP712, respectively. Mutant strains BP703, BP706, and BP712 were created by introducing the mobilizable plasmids pBP703, pBP706, and pBP712, respectively, into strain FD by

TABLE 1 Plasmids and strains

Strain or plasmid	Description or relevant characteristic(s)[a]	Source or reference
Strains		
FD	*A. variabilis* ATCC 29413 wild-type parent strain	66
BP703	pBP703 integrated into the chromosome of strain FD via double recombination, creating a stem-loop structure at the transcription-processing site in the *nifUH* intergenic region similar to the WT using a different nucleotide sequence	This study
BP706	pBP706 integrated into the chromosome of strain FD via double recombination, creating a mutation in the stem-loop structure at the transcription-processing site in the *nifUH* intergenic region	This study
BP712	pBP712 integrated into the chromosome of strain FD via double recombination, creating a deletion in the promoter for the antisense transcript in the *nifUH* intergenic region	This study
BP750	pBP750 inserted into the *frtBC* region of FD, creating a wild-type *nifU1-lacZ* fusion strain	This study
BP751	pBP751 inserted into the *frtBC* region of FD, creating a wild-type *nifU1-lacZ* fusion strain	This study
BP752	pBP752 inserted into the *frtBC* region of FD, creating a wild-type *nifUH1-lacZ* fusion strain	This study
BP753	pBP753 inserted into the *frtBC* region of FD, creating a wild-type *nifUH1-lacZ* fusion strain	This study
JU408	Double recombinant of pJU408 conjugated into FD to yield a deletion of the 5′ end of *nifH1*	This study
JU420	Double recombinant of pJU397 conjugated into JU408	This study
JU422	Double recombinant of pJU399 conjugated into JU408	This study
JU423	Double recombinant of pJU400 conjugated into JU408	This study
JU472	Fusion of *lacZ* to a 751-bp *nifU1-nifH1* fragment, placing *lacZ* at the start of *nifH1*	39
Plasmids		
pBP609	Vector with a promoterless *lacZ* for promoter fusions and an internal *frtABC* fragment for recombination; Km^r	This study
pBP700	2.35-kb *nifUH1* intergenic region with the stem-loop structure restored to WT structure using different nucleotides, made with two PCR products (made from primer sets nifHLoop1-L/nifHLoop1-R and nifHResLoop2-L/nifHLoop2-R) and inserted into PstI/KpnI sites of pUC18	This study
pBP701	2.35-kb *nifUH1* intergenic region with the stem-loop structure mutated, made with two PCR products (made from primer sets nifHLoop1-L/nifHLoop1-R and nifHMutLoop2-L/nifHLoop2-R) and inserted into PstI/KpnI sites of pUC18	This study
pBP703	6-kb SacI fragment of pRL2948a cloned into the SacI site on pBP700; Ap^r Cm^r Em^r	This study
pBP706	6-kb SacI fragment of pRL2948a cloned into the SacI site on pBP701; Ap^r Cm^r Em^r	This study
pBP711	2.9-kb fragment containing the *nifUH1* intergenic region with a deletion in the promoter of an antisense *nifU1* transcript, made with two PCR products (made from primer sets antiloopmut-1/antiloopmut-2 and antiloopmut-3/antiloopmut-4) and inserted into PstI/KpnI sites of pUC18	This study
pBP712	6-kb SacI fragment of pRL2948a cloned into the SacI site on pBP711, with the *sacB* gene transcribed in the same direction as *nifH1*; Ap^r Cm^r Em^r	This study
pBP750	264-bp *nifU1* fragment (made from primers pnifUH-L4 and pnifU-R1) inserted into the BglII/SmaI sites of pBP609	This study
pBP751	457-bp *nifU1* fragment (made from primers pnifUH-L4 and pnifU-R2) inserted into the BglII/SmaI sites of pBP609	This study
pBP752	550-bp *nifU1-nifH1* fragment (made from primers pnifUH-L4 and pnifU-R3) inserted into the BglII/SmaI sites of pBP609	This study
pBP753	628-bp *nifU1-nifH1* fragment (made from primers pnifUH-L4 and pnifU-R4) inserted into the BglII/SmaI sites of pBP609	This study
pEL1	4.1-kb BamHI region from 33D12 containing *nifSUHD1* (67) in pUC118	This study
pJU375	Nm^r cassette from pBP285 in EcoRV on pBP285	This study
pJU376	Fragment of pRL2948 cut with EcoRV, containing *sacB* and a Cm^r cassette inserted into the SmaI site of pJU375	This study
pJU378	PCR product made from pEL1 using nifH69L/nifH69R and then ligated to circularize	This study
pJU380	PCR product made from pEL1 using nifH95L/nifH95R and then ligated to circularize	This study
pJU381	PCR product made from pEL1 using nifH120L/nifH120R and then ligated to circularize	This study
pJU397	Insertion of *sacB* and the Cm^r cassette from pRL2948 cut with SacI into the SacI site on pJU378	This study
pJU399	Insertion of *sacB* and the Cm^r cassette from pRL2948 cut with SacI into the SacI site on pJU380	This study
pJU400	Insertion of *sacB* and the Cm^r cassette from pRL2948 cut with SacI into the SacI site on pJU381	This study
pJU408	377-bp 5′ *nifH1* fragment removed from pJU376 using partial AgeI and religating of the vector	This study
pRL2948a	Source of mobilization site, *oriT*, and *sacB* gene, which confers sucrose sensitivity; Cm^r Em^r	C. P. Wolk
pUC18	Cloning vector; Ap^r	68

[a] Cm^r, chloramphenicol resistance; Tc^r, tetracycline resistance; Ap^r, ampicillin resistance; Sm^r, streptomycin resistance; Km^r, kanamycin resistance; Sp^r, spectinomycin resistance; Em^r, erythromycin resistance; Nm^r, neomycin resistance.

conjugation, as previously described (50). Single recombinants were selected by Em^r, followed by isolation of double-recombinant mutants using *sacB* selection (51) on AA plates supplemented with 5 mM NH_4Cl, 10 mM TES, 10% sucrose. PCR was used to verify that there were no wild-type copies of the region of interest. Further, the *nifUH1* region was sequenced in BP703, BP706, and BP712 to verify the mutations.

Strains JU420, JU422, and JU423 were constructed as follows. A 4.1-kb BamHI region from 33D12 containing *nifSUHD1* was cloned in pUC118,

TABLE 2 Primers

Oligonucleotide	Sequence (5′→3′)
DNA	
antiloopmut-1	TATACTGCAGCTTAAACAAATATGGCATCTGTGCGT
antiloopmut-2	TATATCTAGACATGATGGGTTCGTTATGTAATTAAGT
antiloopmut-3	TATATCTAGACTGTAGAGCGATCGCCCC
antiloopmut-4	AAACACCACGGTTTAGAGGGAACAGAAC
antinifH111	TAGTCATTAGTCATTAGTCAATGGTCAT
antinifH164	CAGATTACGCGATCGCATTAA
antinifH216	CGTGTGGCTCCTGTTCTAGTAGTACA
antinifH245	CGATATTGTCAAAGTAGTACTGCAAGG
antinifH352	CTCACCAACGTGCAGAAGATT
antinifH-5′	ATGATGGGTTCGTTATGTAATTAAGT
nifUH-R20	CTACAGAAAAACCGGTAGAATTATTGTTC
nifUH-R21	CTATGGCTGTGAGGGGTTTGTAGAA
nifHLoop1-L	TATACTGCAGAGATTGTTGACTCCCGCTTCCAGAC
nifHLoop1-R	TATATCTAGAGTATGCTGAGAAAAACCGGTAGAATTATTGTTCATGAT
nifHMutLoop2-L	TATATCTAGACCCTCTTCGGCGACGTTCTACAAA
nifHResLoop2-L	TATATCTAGACCCTCTTCTCTAGGTATGCTGAAACCCCTCACAGCCATAGCTCAACAG
nifHLoop2-R	AAACACCACGGTTTAGAGGGAACAGAAC
nifH302-L10	ATTATCTAGACCTAGTAGTAGAAGCAGTTTAGTCATTAGTCA
nifH302-L11	ATTAGCTAGCCCTAGTAGTAGAAGCAGTTTAGTCATTAGTCA
nifH1out	CCATAGCTGCAAGGGTGTTT
nifH-RTL	ACAGGCGTGAGATCCAAACA
nifH-RTR	CATCAAACGGGTGGAGTCAG
pnifUH-L4	AATAGATCTGAAAATAAGGTACGTCGCATAG
pnifU-R1	ATTACCCGGGCTTCTTCGTCTAATACTTTTTGAATGAGG
pnifU-R2	ATTACCCGGGACTAATGACTAAACTGCTTCTACTACTAGGCTG
pnifU-R3	TATACCCGGGATGTAATTAAGTGATGAGTGCTGAGTCC
pnifU-R4	AATTCCCGGGGTTTGTAGAACGTCGCCGAAGAG
P1 oligo B	CCTGTAGAACGAACACTAGAAGA
qnifB1-L	AATGGACGAAAAGCTCCAAGAAC
qnifB1-R	GTGCTGCTTCTTCTGGTGTGAGT
qnifD-L	GTTGCGGTTACTGGTCTTGGTC
qnifD-R	CACCACGGTTTAGAGGGAACAG
qnifE (Sept)-L	CGCCTGTGCTGGTAATTCTTG
qnifE (Sept)-R	AGACAAATACCGCCGATGGAT
qnifHloop-L	TGGACTATGGACTCAGCACTCA
qnifHloop-R	TTGGATCTCACGCCTGTTGAGC
qnifH-F	ACCAAGGTCAAGAGTACCGTGCAT
qnifH-R	ATTTGGTAGCTTCTGCGGGCTTAC
qnifK-L	ACACACCTCAGCCGTCACTACA
qnifK-R	CCGATAACCTCAGCCATACAGG
qnifS1-L	CTTTGGTGGACAACTGGGAAAG
qnifS1-R	GGGTTGTAATGATGTGGCGTTT
qnifX-L	TCGCACTTCGGTTCTGCTAAA
qnifX-R	CCCACCAATAGCGACGACATA
qrnpB-F	TGGATAACTTCCAGTGCGAGCGAT
qrnpB-R	TCTTACCGCACCTTTGCACCCTTA
nifD-RPE1	CGAAAGAGTTGATACCAGTTACACCA
nifD-RPE3	GGCTGATGTGAATCATGTCCTTAATAG
nifK1-R	CGCCAAGTTAGTGATCAAGGAAGT
qAva3931-R	CGTTTCGCTCATCTTGTTTGC
nifE-PCR3	AATCCTTTCCCTAGCCCCT
nifHb69-L	GCTAGATCTCGTGAGATCCAAACACAAAGACCGACCAACTA
nifHb69-R	GCTAGATCTGAGCTATGGCTGTGAGGGGTTTGTAGAACGT
nifHb95-L	GCTAGATCTCAAACCCCTCACAGCCATAGCTCAACAGGCGT
nifHb95-R	GCTAGATCTGACGCCGAAGAGGGGGCGATCGCTCTACA
nifHb120-L	GCTAGATCTGATCGCCCCCTCTTCGGCGACGTTCT
nifHb120-R	GCTAGATCTCAGAAAAACCGGTAGAATTATTGTTCATGATGGG
RNA primer RNAoligo09	AUAUGCGCGAAUUCCUGUAGAACGAACACUAGAAGAAA

to create pEL1. A SmaI fragment containing the neomycin resistance (Nm^r) cassette from pBP285 was inserted into the *nifU1* gene of pEL1 at the EcoRV site to create pJU375. pJU376 was constructed by inserting the 5-kb EcoRV fragment of pRL2948 containing *sacB* and the chloramphenicol resistance (Cm^r) cassette into the SmaI site of pJU375. pJU376 was partially digested with AgeI to remove a 377-bp fragment containing the 5′ end of *nifH1* and religated to create pJU408. This plasmid was introduced into FD by conjugation to create a deletion of the 5′ end of *nifH1* via double recombination, strain JU408, using *sacB* selection as described above. To generate the mutations in JU420, JU422, and JU423, PCR was performed on pEL1 using the following primer pairs: JU420-nifH69L/JU420-nifH69R, JU422 nifH95-L/JU422 nifH95-R, and JU423-120L/JU423-120R. These initial PCR fragments were ligated to circularize into a plasmid. The plasmids were named pJU378, pJU380, and pJU381, respectively. pJU397, pJU399, and pJU400 were made by inserting *sacB* and the Cm^r cassette from pRL2948 cut with SacI into the SacI site in pJU378, pJU380, and pJU381, respectively. Plasmids pJU397, pJU399, and pJU400 were conjugated into JU408, and double recombinants were recovered using sucrose selection, and verified by screening for Nm sensitivity to generate JU420, JU422, and JU423, respectively. The mutations in the *nifUH1* region were verified by sequencing.

Fusions of *nifU1*::*lacZ* and *nifUH1*::*lacZ* (pBP750 to pBP753 and pJU472) were made by cloning various PCR fragments, amplified from FD DNA, into the BglII/SmaI sites in pJU411 or pBP609, as described in Table 1. Plasmids pJU411 and pBP609 have an internal fragment of the fructose transport genes, *frtABC* (52), that allows screening for single recombinants at the *frtABC* locus, which results in a mutant that cannot use fructose. Promoter fragments were sequenced to verify that they contained no mutations. Recombinations of these plasmids with promoter fragments fused to *lacZ* into the *frt* region of *A. variabilis* by single crossover following conjugation (53) were identified by screening for colonies that were unable to grow in the dark with fructose (BP750 to BP753 and JU472).

RNA isolation and analysis. RNA decay was measured as previously described (46). Strains were grown in AA/8 supplemented with 5 mM NH_4Cl and 10 mM TES, pH 7.2, and 50-ml cultures at an OD_{720} of 0.2 to 0.3 were washed free of fixed nitrogen and grown for 24 h with aeration to induce heterocysts and nitrogen fixation. Cells were removed at 24 h for the 0-h time, and then, 100 $\mu g\ ml^{-1}$ rifampin was added to the cultures to inhibit new transcription. At 10, 20, 30, 45, and 60 min after the addition of rifampin, 50 ml of cells was chilled quickly by pouring over ice in 2 50-ml centrifuge tubes, harvested, and frozen. RNA was isolated using Tri-Reagent (Sigma), as previously described (39), and subjected to DNase digestion (Turbo DNA-free kit; Ambion).

Reverse transcription-quantitative PCR (RT-qPCR) was used to determine the quantities and decay rates of transcripts. cDNA was made from 40 ng of RNA using Bio-Rad iScript Reverse Transcription Super Mix (catalog no. 170-8841) in a 10-μl reaction mixture. The cDNA was diluted 1:20 to 0.2 ng μl^{-1} for qPCR. qPCRs were done using Bio-Rad SsoAdvanced SYBR Green SuperMix (catalog no. 1725261) in a 10-μl reaction volume and contained 0.8 ng cDNA, 5 pmol of gene-specific primers, and 1× reaction supermix. The following gene-specific primer pairs were used: *rnpB*, qrnpB-F/qrnpB-R; *nifB1*, qnifB1-L/qnifB1-R; *nifS1*, qnifS1-L/qnifS1-R; *nifH1*, qnifH1-L/qnifH1-R; *nifD1*, qnifD-L/qnifD-R; *nifK1*, qnifK-L/qnifK-R; *nifE1*, qnifE (Sept)-L/qnifE (Sept)-R; and *nifX1*, qnifX-L/qnifX-R. Additionally, the following primer pairs were used to determine the stability around the predicted stem-loop structure: loop 5′, antinifH111/antinifH-5′; loop-span, qnifHloop-L/qnifHloop-R; and loop 3′, nifH-RTL/nifH-RTR. In some experiments, strand-specific cDNA was made from 50 ng of RNA using SuperScript III reverse transcriptase from Invitrogen. The manufacturer's recommended protocol was followed, using gene- and strand-specific primers rnpB-R and antinifH111 for looking at the expression of antisense RNA in BP712 and the WT. Additionally, we made strand-specific cDNA to look at the 3′ end of the antisense *sava4870.1* transcript, using rnpB-R and antinifH111, antinifH164, antinifH216, antinifH245, or antinifH352. The reaction temperature for strand-specific cDNA was 52°C for 1 h, followed by an inactivation step at 70°C for 15 min; the cDNA was diluted 1:10 for qPCR. The qPCRs were done using Bio-Rad SsoAdvanced SYBR Green, as described above, using 4 μl of diluted strand-specific cDNA. The following primer pairs were used to amplify antisense RNA products in FD and BP712: *rnpB*, qrnpB-F/qrnpB-R; "antinif," antinifH-5′/antinifH111; R20, nifUH-R20/antinifH111; R21, nifUH-R21/antinifH111; and *nifH*, nifH-RTR/nifH-RTL. Additionally, the following primer pairs were used to identify the 3′ end of the *sava4870.1* antisense transcript: 111 bp, antinifH-5′/antinifH111; 164 bp, antinifH-5′/antinifH164; 216 bp, antinifH-5′/antinifH216; 245 bp, antinifH-5′/antinifH245; and 352 bp, antinifH-5′/antinifH352. The qPCR program for all reactions was denaturation at 95°C for 1 min, followed by 40 cycles at 95°C for 10 s, 55°C for 30 s, and 72°C for 30 s. Data analysis was performed using Bio-Rad CFX Manager 3.0. The averages and standard deviations of triplicate biological samples are shown. The RNA half-life was calculated using time points after the addition of rifampin that best represented 2-fold decay, as described previously (46).

5′ rapid amplification of cDNA ends (RACE) was performed as described previously (46). Briefly, 20 μg of DNase-free RNA was divided into two reaction mixtures; half was untreated, while half was treated with 20 U of tobacco acid pyrophosphatase (TAP) (Epicentre, Madison, WI). The RNA adapter RNAoligo09 (150 pmol) was added to each tube and was extracted with organic solvents and ethanol precipitated. The pellet, resuspended in 14 μl of water, was heated to 90°C for 5 min and ligated to the adapter overnight at 17°C using T4 single-stranded RNA ligase (NEB). The ligated RNA was extracted with organic solvents and ethanol precipitated with 2 pmol of cDNA primers, resuspended in 20 μl of water, and reverse transcribed using Superscript III (Invitrogen) according to the manufacturer's protocol using the following primers: *nifD*, nifD1-RPE1; *nifK*, qnifK-R; and *Ava_3931*, nifE-PCR3. PCR was performed using the left primer P1 oligo B and the following right primers: *nifD*, nifD-RPE3; *nifK*, nifK1-R; and *Ava_3931*, qAva3931-R. PCR bands were excised and sequenced to determine the 5′ ends.

β-Galactosidase assays. β-Galactosidase assays were done in 96-well plates with biological quadruplicate samples and a modification of the standard *Escherichia coli* assay (54) for cyanobacteria, as described previously (46), using cells permeabilized in 0.05 M $NaPO_4$, pH 7.4, 0.1% Sarkosyl, 160 $\mu g\ ml^{-1}$ orthonitrophenyl-β-galactoside. Samples were read at OD_{420} and OD_{665}. Activity was determined essentially as described by Miller (54) but using the following formula: $1{,}000 \times \{OD_{420}$ of sample $- OD_{420}$ of blank $- [1.58 \times (OD_{665}$ of sample $- OD_{665}$ of blank)]$\}/(OD_{720}$ of sample $- OD_{720}$ of blank$) \times t$ (in minutes). The averages and standard deviations of triplicate biological samples are shown.

Acetylene reduction assays. Nitrogenase activity was measured *in vivo* by acetylene reduction assays. Five-milliliter aliquots of cultures at an OD_{720} of about 0.15 were added to 16-ml Hungate tubes. The tubes were sealed with gas-tight stoppers, injected with 1.0 ml acetylene gas, and shaken at 30°C in the light for 60 min. Samples (250 μl) of headspace gas were injected into a Shimazu gas chromatograph equipped with a 6-ft Poropak N column. The average and standard deviation of triplicate biological samples are shown.

Naming the antisense RNA. We followed the recommended convention for naming of small RNAs, which is to begin with the letter "s," then the three-letter genome identifier (ID) used in the KEGG database, "ava," and then the number that indicates its genomic location to the nearest kilobase plus 1 (55). As recommended by the Bacterial Small Regulatory RNA Database (BSRD), we added a period and the number "1" at the end to indicate the number of small RNAs (sRNAs) identified in this location (which is currently one). Thus, the name is *sava4870.1* based on a transcription start site at position 4869891 (kb 4869 + 1 = 4870).

Bioinformatic analysis. DNA sequences were aligned using Clustal Omega, followed, where indicated, by manual alignment (56). Predicted

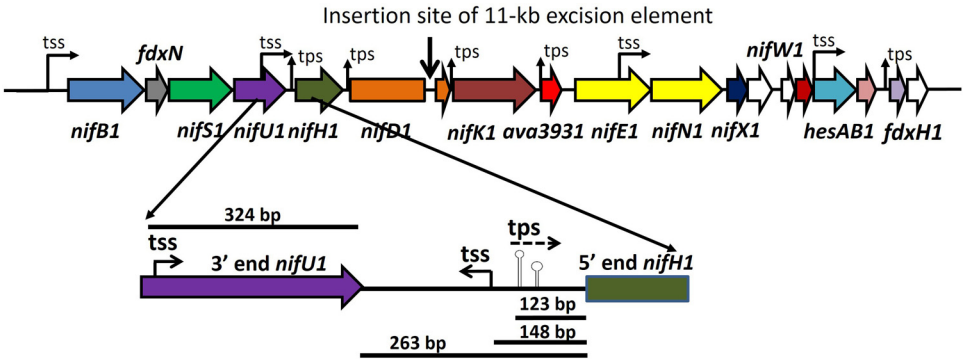

FIG 1 Map of the *nif1* gene cluster showing tss and tps. The 263-bp intergenic region between *nifU1* and *nifH1* is shown, with the predicted stem-loop structures (bottom) just downstream of the tps for *nifH1* at −123 from the start of *nifH1* and the tss for the antisense RNA that begins at −148 from *nifH1*. The processing site upstream of *nifD1* is at −44 from the *nifD1* start site. The processing site upstream *nifK1* is at −131 from the *nifK1* start site. The processing site upstream of *Ava_3931* is near the start of the gene.

secondary structures and the Δ*G* values for those structures were found using m-fold, with the default settings for the program (57).

RESULTS

The tps is required for *nifH1* expression. We have shown previously that the large *nif1* cluster encoding the heterocyst-specific Mo nitrogenase is controlled primarily by the first promoter of the cluster, located 328 bp upstream of *nifB1*, with additional weak promoters inside *nifU1*, inside *nifE1*, and upstream of *hesA1* (Fig. 1) (7, 39, 46). A smaller *nifH1* transcript is made by processing of the longer transcript at a transcriptional processing site (tps) located 123 bp upstream of *nifH1* at the base of a predicted stem-loop structure. Additional processing sites were identified between *nifH1* and *nifD1*, between *nifD1* and *nifK1*, and between *nifK1* and *Ava_3931* (see below) and between *hesB1* and *fdxH1* (46).

We have shown previously that a promoter in the *nifU1* gene provides weak, heterocyst-specific expression of *nifH1* independent of the primary *nifB1* promoter (39, 46); however, the importance of sequences in the *nifUH1* intergenic region for *nifH1* expression is not known. We constructed fusions of the *nifU1* internal promoter and various-length regions of the *nifUH1* intergenic region to a promoterless *lacZ* in strains BP750, BP751, BP752, and BP753 (Fig. 2A). There was only basal-level expression of *lacZ* from the *nifU1* promoter in fragments that lacked the processing site located 123 bp upstream of *nifH1* (strains BP750, BP751, and BP752); however, strain BP753, with *lacZ* fused to the *nifU1* internal promoter at a site 43 bp downstream from the processing site, had levels of β-galactosidase similar to those of the positive control, JU472, in which *lacZ* was fused at the start of *nifH1* (39). This result is consistent with expression of *lacZ* from the weak *nifU1* promoter (Fig. 2B), suggesting that the processing site is important for expression of *nifH1*.

The predicted stem-loop structure is important for *nifH1* transcript processing and stability. The sequence near the 5′ end of the processed *nifH1* transcript is conserved among many heterocyst-forming cyanobacteria, and that sequence forms the 5′ region of the predicted stem in the stem-loop. The stem-loop structure is also conserved, although the structure is variable in size and shape among the cyanobacterial strains (see Fig. S1B in the supplemental material; see also sequence data in reference 69). We have shown previously that the *nifH1* transcript is much more stable than the *nifU1* transcript (46); therefore, we were interested in the role of the stem-loop structure in the processing and stability of the *nifH1* transcript.

In order to determine the importance of the predicted stem-loop region in the stability of the *nifH1* transcript, we measured the stability of transcripts in the *nifU1-nifH1* intergenic region by RT-qPCR from RNA extracted at various times after the addition of rifampin to block initiation of transcription. Primers were chosen to yield a product from transcripts directly upstream of the

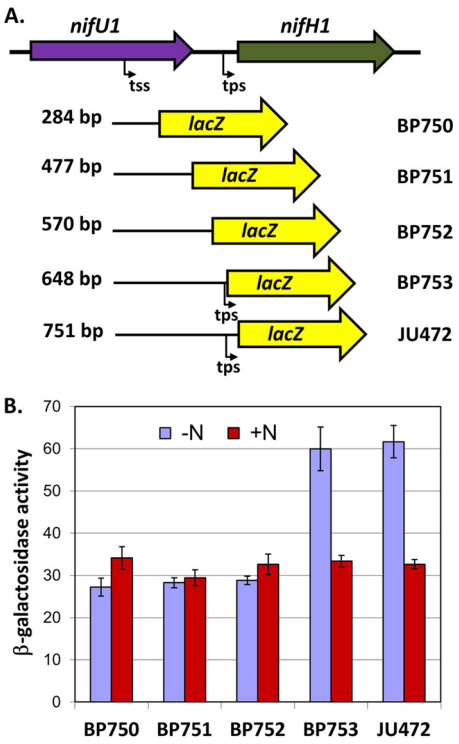

FIG 2 Expression from the *nifU1* internal promoter. (A) Construction of the *nifU1*::*lacZ* fusion strains. (B) β-Galactosidase activity, expressed in Miller units, of the strains grown with fixed nitrogen (+N) or 24 h after removal of fixed nitrogen (−N). In BP753, *lacZ* is fused 43 bp downstream from the tps, and in JU472, it is fused 146 bp downstream from the tps (39). The error bars indicate standard deviations.

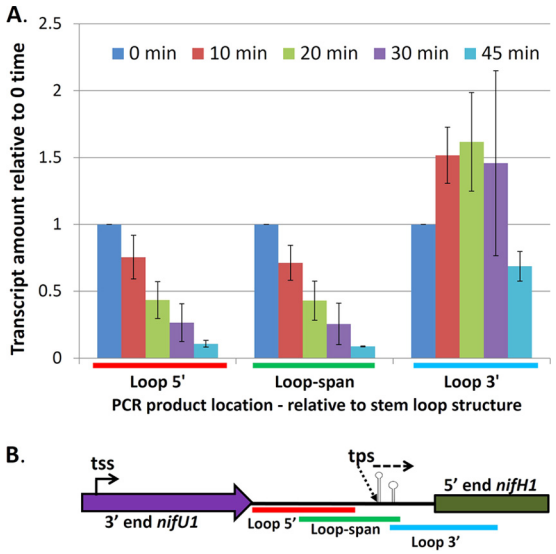

FIG 3 Stability of transcripts near the tps of *nifH1*. (A) Transcript stability was determined by measuring transcript amounts by RT-qPCR from RNA collected at 10, 20, 30, 45, and 60 min after the addition of rifampin to cells that had been induced to fix nitrogen by the removal of fixed nitrogen from the medium 24 h before the start of the experiment (zero time). Primers used for RT-qPCR amplified a region upstream from the tps (Loop 5′), a region spanning the tps (Loop-span), or a region downstream from the tps (Loop 3′). The data are based on triplicate biological samples. The error bars indicate standard deviations. (B) Map showing the locations, relative to the stem-loop structures, of Loop 5′, Loop-span, and Loop 3′ products.

predicted stem-loop structure (Loop 5′), spanning the stem-loop structure (Loop-span), or directly downstream of the stem-loop structure (Loop 3′). Transcripts in the Loop 5′ region and the Loop-span region had a half-life of about 12 min, with decay evident immediately after the addition of rifampin (Fig. 3). In contrast, the transcript in the Loop 3′ region was much more stable, lasting longer than 30 min (Fig. 3), and it showed the transient increase in transcript after rifampin addition that was shown previously to be characteristic of the transcripts downstream from RNA-processing sites in the *nif1* cluster (46). These data provide strong evidence that the region that comprises the stem-loop structure confers stability of the *nifH1* transcript.

To determine the importance of the sequence of the predicted stem-loop versus the secondary structure, two mutations were created that changed the sequence in this region. One mutation abolished the predicted stem-loop structure (strain BP706), while the second mutation changed the sequence in the region compared to the wild-type strain but maintained a stem-loop structure very similar to that of the wild-type strain with a similar Δ*G* (strain BP703) (Fig. 4A). The effects of these mutations on processing of the transcript were determined by 5′ RACE. No processed transcript was detected in RNA isolated from strain BP706, which lacked the predicted stem-loop structure. A weak product was detected in RNA isolated from strain BP703, which had a predicted stem-loop structure with altered nucleotides, and the sequence of this product showed that the 5′ end corresponded to the mutation created in BP703 (Fig. 4B). Thus, the stem-loop structure is important in RNA processing, and processing is impaired if the sequence in the predicted stem-loop region is incorrect. However, the fact that the mutant BP703 lacks wild-type levels of tran-

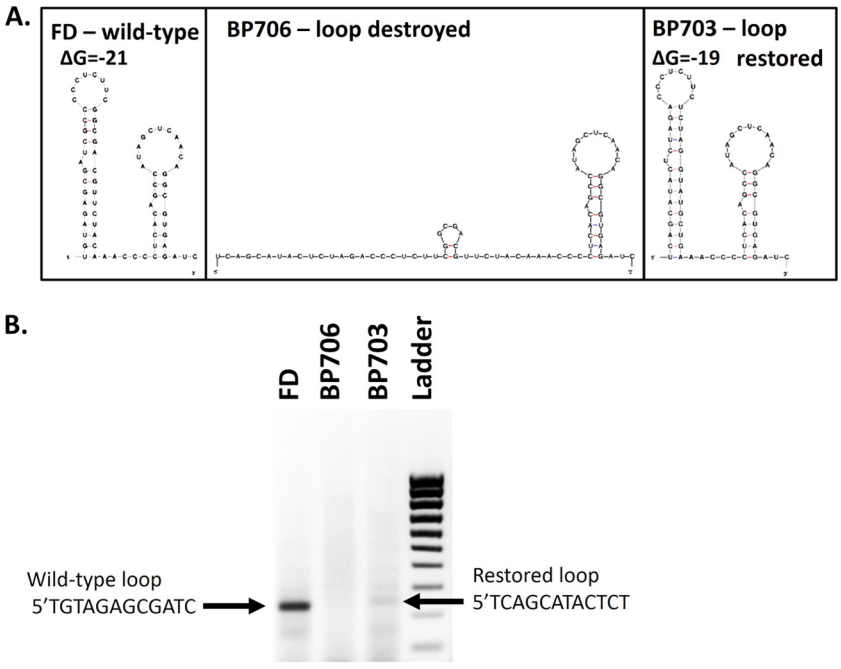

FIG 4 Mapping *nifH1* transcript 5′ ends. (A) Predicted secondary structures in the region just downstream of the transcriptional processing site for *nifH1* for the wild-type strain and the two mutants; one mutant abolished the first stem-loop (BP706), while the second mutant restored the stem-loop with a different sequence (BP703). The Δ*G* values represent only the first stem-loop structure, not both loops. (B) RNA isolated from cells grown without fixed nitrogen for 24 h was analyzed by 5′ RACE in strains FD, BP706, and BP703. Because the 5′ end of *nifH1* is a processed site, the 5′ RACE was done without TAP treatment of the RNA. The bands indicated by the arrows for FD and BP703 were recovered from the gel and sequenced to determine the tps of *nifH1* in the strains. The sequence for BP703 confirmed the stem-loop structure shown in panel A.

TABLE 3 Half-lives of *nif1* transcripts in wild-type (FD) and mutant (BP706 and BP703) strains

Gene	Half-life[a] (min)		
	FD	BP706	BP703
nifB1	12.3 ± 2.2	14.3 ± 4.7	14.2 ± 4.6
nifS1	14.8 ± 4.8	15.7 ± 3.5	11.5 ± 1.1
nifH1	33.8 ± 7.7	19.7 ± 5.1	24.15 ± 7.8
nifD1	22.2 ± 4.1	11.2 ± 4.7	14.3 ± 2.8
nifK1	16.7 ± 3.5	13.9 ± 4.7	14.7 ± 4.5
nifE1	7.4 ± 1.3	6.9 ± 1.8	7.3 ± 2.1
nifX1	12.3 ± 2.1	15.1 ± 4.2	13.7 ± 3.2

[a] The half-lives were calculated from the decay of transcripts at 10, 20, 30, 45, and 60 min after the addition of rifampin to cells.

script suggests that the sequence, as well as the stem-loop structure, is important in normal transcript processing.

The effects of these mutations on the stability of genes in the *nif1* cluster were determined by RT-qPCR with RNA extracted at various times after the addition of rifampin to block initiation of transcription. The major effect of the mutation in BP706 that destroyed the predicted stem-loop structure was on the *nifH1* and *nifD1* transcripts, which had much shorter half-lives than the wild-type strain, with little effect on the other *nif1* genes tested (Table 3). The restoration of a stem-loop structure with altered nucleotides in strain BP703 resulted in increased half-lives for *nifH1* and *nifD1* compared to BP706, although they were not as long as those for the wild-type strain (Table 3). These results suggest that while the predicted stem-loop structure plays a role in stability, other factors, including the sequence, are probably also important.

The effects of the predicted stem-loop mutations on transcript abundance, nitrogenase activity, and growth rate were determined for FD, the wild-type strain; for BP703, lacking a predicted stem-loop structure; and for BP706, with a stem-loop structure with altered bases. Loss of the predicted stem-loop structure in mutant BP706 resulted in loss of about 90% of the *nifH1* transcript and about two-thirds of the *nifK1* transcript (Fig. 5A), with less effect on transcripts for *nifE1* and *nifX1* farther downstream. Restoration of the predicted stem-loop in BP703 resulted in a 2- to 3-fold increase in transcript levels for both *nifH1* and *nifK1* compared to BP706 and essentially normal levels of transcripts for *nifE1* and *nifX1* (Fig. 5A). Mutant BP706 showed only about 25% of the wild-type levels of nitrogenase activity, while restoration of a predicted stem-loop in BP703 partially restored nitrogenase (Fig. 5B), consistent with the increase in *nifH1* transcript in this strain (Fig. 5A). Growth data confirmed that the complete loss of the predicted stem-loop in BP706 was accompanied by slower growth and that restoration of a predicted stem-loop increased the growth rate to about 75% of the wild-type rate (Fig. 5C). Thus, the loss of the stem-loop structure resulted in impaired growth that correlated with reduction in nitrogenase activity and loss of transcript, but restoration of a stem-loop structure with an altered sequence only partially restored growth, nitrogenase activity, and transcript abundance. Interestingly, the reduction of *nifH1* transcript to only 10% of wild-type levels in the stem-loop mutant, BP706, reduced the nitrogenase activity only about 75% and the growth rate only about 50% compared to wild-type cells.

Mutations in the predicted stem-loop structure that are highly conserved among heterocystous cyanobacteria were also tested to determine their effects on the transcript level, nitrogenase activity, and growth. A 5-bp alteration in mutant strain JU420 that affected only the shorter downstream 3′ stem-loop structure (Fig. 6A) had no effect on nitrogenase activity (Fig. 6B) or on growth (not shown) but resulted in a decrease in the *nifH1* transcript level to about 50% of the wild-type level (Fig. 6C). An 8-bp alteration in strain JU422 that changed the sizes of both stem-loop structures and the spacing between them and increased the Δ*G* of the first predicted stem-loop structure (Fig. 6A) decreased nitrogenase activity, reflecting the greater reduction in the *nifH1* transcript level than in JU420 (Fig. 6B). A 6-bp alteration in mutant strain JU423, which altered the sequence very near the processing site and greatly increased the Δ*G* of the first predicted stem-loop structure (Fig. 6A), had the greatest effect, with a 5-fold reduction in *nifH1* transcript levels and a 40% reduction in nitrogenase activity compared to the wild-type strain (Fig. 6B and C). All three mutants gave 5′ RACE products that appeared to be the same size (Fig. 6D); however, the sequences of the 5′ ends of the transcripts revealed

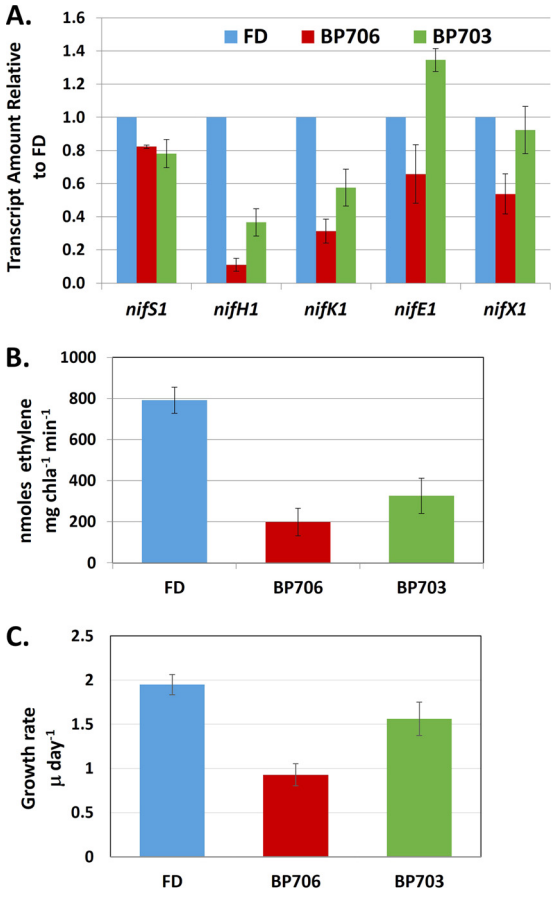

FIG 5 Analysis of mutants in the *nifU1-nifH1* intergenic stem-loop structure. (A) The amounts of *nifB1*, *nifS1*, *nifH1*, *nifK1*, *nifE1*, and *nifX1* transcripts in strains FD, BP706, and BP703 were measured by RT-qPCR in RNA harvested from cells 24 h after the removal of fixed nitrogen. The amounts of *nifS1*, *nifH1*, *nifK1*, *nifE1*, and *nifX1* transcripts were normalized to those of *nifB1* and compared to the wild-type strain, FD. (B) Nitrogenase activities of the wild-type strain, FD, and mutants BP706 and BP703 were measured by acetylene reduction 24 h after the removal of fixed nitrogen from the medium. Ethylene values were normalized to chlorophyll *a* (chla). (C) Growth of the wild-type and mutant strains was measured in cells grown for several generations in the absence of fixed nitrogen prior to the assay. The error bars indicate standard deviations.

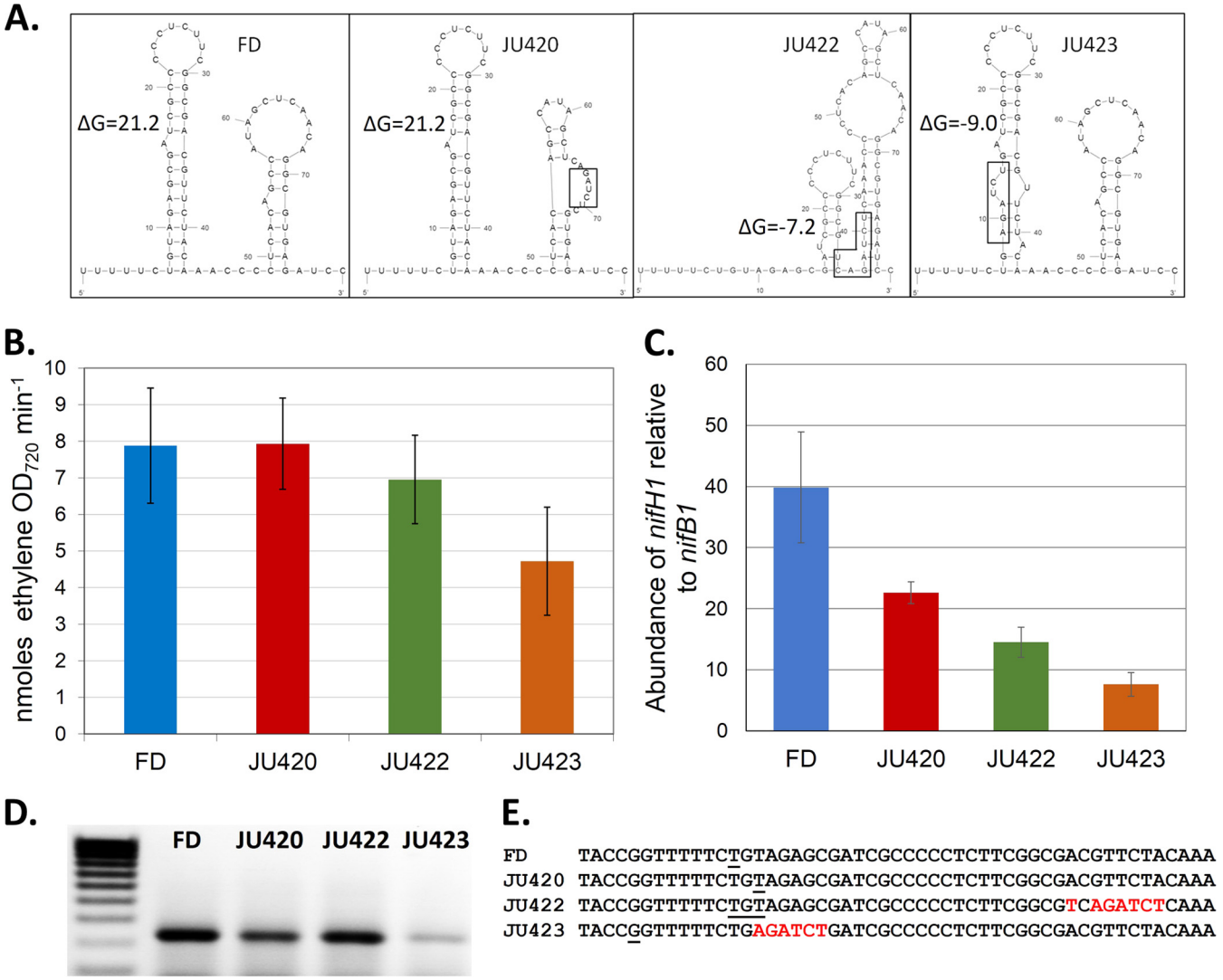

FIG 6 Effects on *nifH1* expression of mutations in the conserved regions of stem-loop structures. (A) Locations of mutations in JU420, JU422, and JU423 and their predicted effects on RNA secondary structure. Δ*G* values are shown for only the first predicted stem-loop structure. The mutations are shown in the boxed regions. (B) The nitrogenase activities of the mutants were measured by acetylene reduction 24 h after the removal of fixed nitrogen from the medium. (C) The amounts of *nifH1* and *nifB1* transcripts were measured by RT-qPCR from RNA harvested from cells 24 h after the removal of fixed nitrogen. The amount of *nifH1* transcript is shown relative to that of *nifB1*. (D) 5′ RACE products for the wild-type strain and each of the mutants. Because the 5′ end of *nifH1* is a processed site, the 5′ RACE was done without TAP treatment of the RNA. (E) Sequences of the 5′ RACE products from panel D. The 5′ ends are underlined, and the mutations in JU422 and JU423 are shown in red (the JU420 mutation is further downstream). The error bars indicate standard deviations.

minor changes in the processed 5′ end for JU420 and multiple ends for JU422, while JU423 had a processing site that was 8 nucleotides upstream from the site in the wild-type strain (Fig. 6E). While these mutations in the conserved areas in the predicted stem-loop region all had effects on *nifH1* transcript levels, like the mutant BP703 with an altered sequence in the 5′ stem-loop (Fig. 3A), the effects on nitrogenase activity and on growth were not severe. In strain JU423, which has a relatively unstable 5′ stem-loop structure and an altered sequence near the processing site (Fig. 6A), the effects were more deleterious, suggesting that the sequence near the processing site, as well as a stable stem-loop structure, is important for proper processing of the transcript, resulting in higher levels of the *nifH1* transcript.

Antisense RNA in the *nifU1-nifH1* intergenic region. The RNA-seq data for *Anabaena* sp. PCC 7120 show small amounts of an antisense RNA with an apparent 5′ end located 148 bp upstream of *nifH* (42), and a primary transcription start site was mapped to that site by RNA-seq using a method that enriched for primary transcripts (43). Therefore, we looked for antisense RNA in this region in *A. variabilis*. Preliminary experiments with various primer sets in the *nifU1-nifH1* intergenic region using strand-specific cDNA identified an antisense transcript with a 5′ end at about 148 bp upstream from the start of *nifH1* (data not shown). Using the nomenclature recommendation for small RNAs (55), we have named this small RNA *sava4870.1* (see Materials and Methods). Primers within the *nifU1* gene (Fig. 7B) were used to determine by RT-qPCR that *sava4870.1* is between 164 and 215 bp in length (Fig. 7A); however, there also appeared to be low-level transcription of antisense RNA that extended further into the *nifU1* gene (Fig. 7A). We compared the amounts of antisense tran-

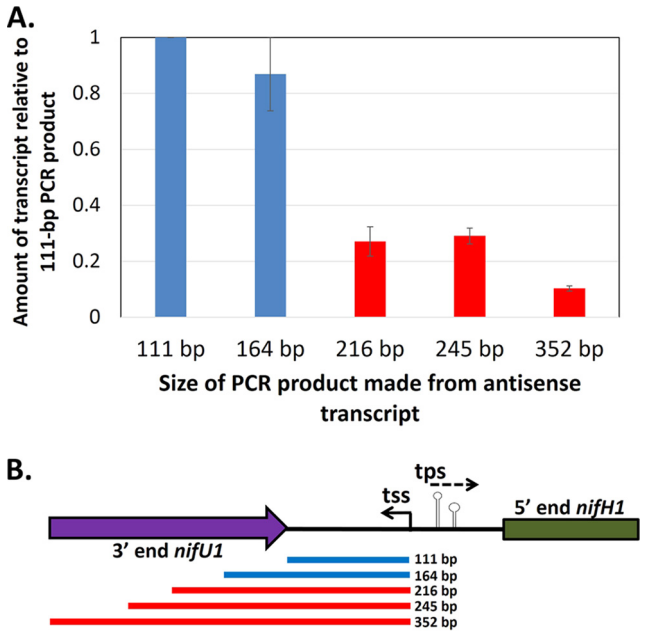

FIG 7 Size of the *sava4870.1* antisense RNA. (A) Antisense RNA was measured by RT-qPCR using strand-specific cDNA. (B) Primer sets used to determine the 3′ end of *sava4870.1*. The tss for *sava4870.1* antisense RNA is located 148 bp upstream of the start of *nifH1* and 25 bp upstream from the tps for *nifH1*. The error bars indicate standard deviations. The colors of the products in panel A match the colors of the lines corresponding to the transcripts in panel B.

script using primers that amplified strand-specific cDNA in cells grown with or without fixed nitrogen. Four sets of primers that amplified the strand-specific cDNA were used (Fig. 8D): (i) *sava4870.1* antisense RNA (labeled "antinif"), (ii) antisense RNA beginning 29 bp upstream of the putative tss for the antisense RNA (R20), (iii) antisense RNA beginning 70 bp upstream of the putative tss for the antisense RNA (R21), and (iv) antisense RNA beginning 64 bp upstream of the start site of *nifH1* to 156 bp into the *nifH1* gene (nifH). The last three served as controls for *sava4870.1* antisense RNA, since they were not within the *sava4870.1* gene. RNA from cells grown without fixed nitrogen showed a 7-fold increase in expression of the antisense transcript for *nifH1* (labeled nifH) compared to the control antisense RNA (R20 and R21) (Fig. 8A); however, there was little or no increase in expression of the *sava4870.1* antisense RNA (antinif) compared to the control antisense RNA (R20 and R21) (Fig. 8A). In contrast, RNA from cells grown with fixed nitrogen showed increased expression of the *sava4870.1* antisense RNA (antinif) compared to the control antisense RNA (R20 and R21) and nifH (Fig. 8B). Expression of the *sava4870.1* RNA (antinif) in cells grown with fixed nitrogen compared to those grown without fixed nitrogen was at least 20-fold higher than the antisense transcripts (R20, R21, and nifH) (Fig. 8C). Thus, the *sava4870.1* transcript is downregulated under conditions of nitrogen fixation, suggesting that it may play a role in inhibiting *nif* gene expression in cells growing with fixed nitrogen.

To determine the effect of loss of the *sava4870.1* transcript, we created a *sava4870.1* promoter mutant, strain BP712, in which a 22-bp deletion in the region immediately upstream of the *sava4870.1* tss was replaced with an XbaI site. This mutation dras-

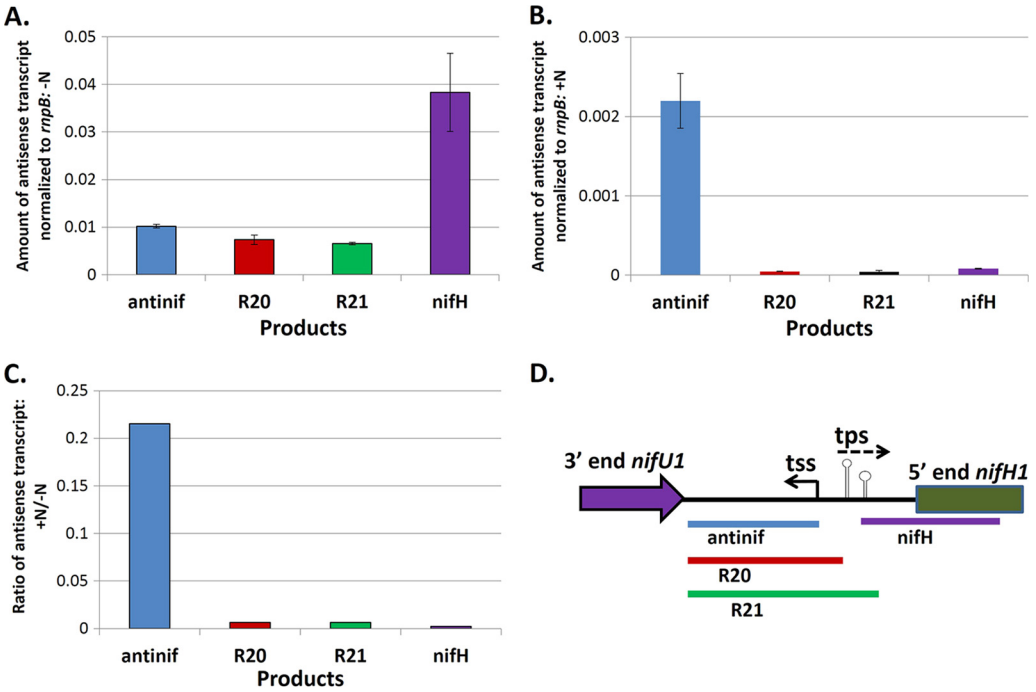

FIG 8 (A and B) Expression of *sava4870.1* antisense RNA in cells grown without (−N) (A) or with (+N) (B) a source of fixed nitrogen. Antisense RNA was measured by RT-qPCR using strand-specific cDNA with primer sets that amplified the regions labeled antinif, R20, R21, or nifH, as shown in panel D. (C) Ratio of antisense RNA expression, +N versus −N, for each region shown in panel D. (D) Map of the *nifU1-nifH1* intergenic region showing the locations of the RT-pPCR products. The error bars indicate standard deviations.

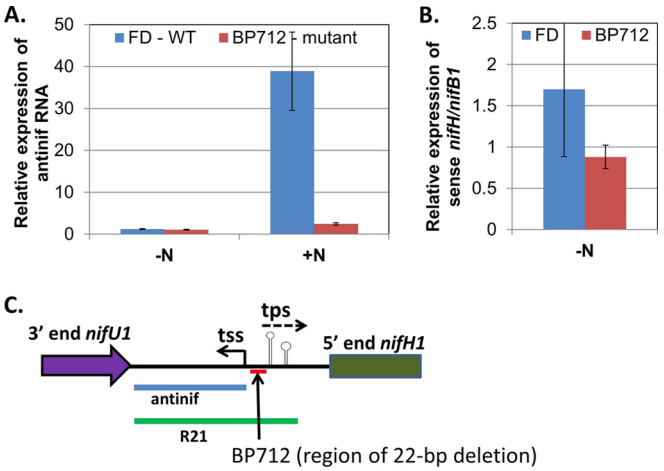

FIG 9 Expression of *sava4870.1* antisense RNA in FD and in mutant BP712. (A) Expression of *sava4870.1* antisense RNA was determined by comparing the amount of antisense RNA (antinif) to the amount of antisense RNA upstream of the antisense region (R21) in the wild-type (FD) and mutant (BP712) strains. (B) Expression of *nifH1* sense RNA was determined by comparing the amount of *nifH1* transcript to the amount of *nifB1* transcript in the wild-type (FD) and mutant (BP712) strains. The error bars indicate standard deviations. (C) Map of the *nifH1* region showing the primers used for the experiment in panel A. The sense primer for *nifH1* (used in the experiment shown in panel B) is at the 3′ end of the gene, outside the region shown.

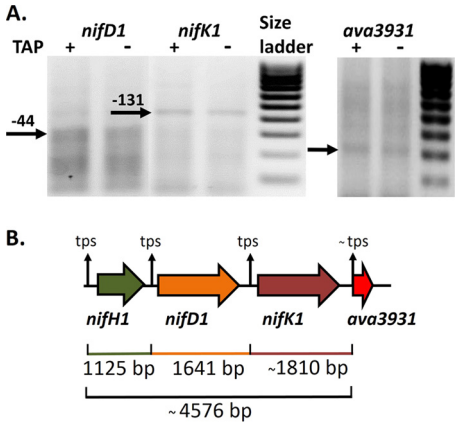

FIG 10 Mapping *nifD1*, *nifK1*, and *Ava_3931* transcript 5′ ends. (A) RNA isolated from cells grown without fixed nitrogen for 24 h was analyzed by 5′ RACE. A band for a processed transcript 44 bp upstream from the start of *nifD1* and a band 131 bp upstream from the start of *nifK1* were present with (+) or without (−) TAP treatment of RNA. A band for a processed transcript near the start of *Ava_3931* was present with or without TAP treatment of RNA; however, we were unable to determine the 5′ end exactly. (B) Map of transcripts for *nifH1*, *nifD1*, *nifK1*, and *Ava_3931* showing the tps and sizes of the deduced transcripts.

tically reduced expression of the *sava4870.1* RNA, as measured by expression of *sava4870.1* in wild-type versus mutant cells grown with fixed nitrogen, but had little effect on expression of the *sava4870.1* RNA in cells grown without fixed nitrogen, consistent with the fact that *sava4870.1* RNA is expressed primarily in cells grown with fixed nitrogen (Fig. 9A). Since the mutation in BP712 also destroyed the region just upstream of the *nifH1* processing site (the promoter deletion extends to −1 relative to the transcriptional processing site), we also determined its effect on expression of the *nifH1* sense transcript. This mutation resulted in a 50% reduction in *nifH1* expression (Fig. 9B), similar to the effect seen for mutations in the predicted stem-loop region, such as JU420 and JU422 (Fig. 6C). The only phenotype associated with the BP712 mutant was a delay of about 24 h before initiation of nitrogen fixation and diazotrophic growth; however, once growth began, the cells appeared to grow normally (data not shown). This phenotype of the BP712 mutant more likely reflects the decrease in expression of *nifH1* sense transcript rather than the loss of the *sava4870.1* transcript, since the antisense RNA is hardly made in the absence of fixed nitrogen. This conclusion is supported by the fact that in BP712 we were not able to detect a 5′ RACE product in RNA from cells grown without fixed nitrogen, suggesting that the *nifH1* transcript is not processed normally in BP712 (data not shown). Further, the half-life of the sense transcript downstream from the transcriptional processing site in BP712, about 10 min, as determined by measuring the Loop 3′ product (Fig. 3A), was very similar to the half-life of the sense transcript upstream of the transcriptional processing site, as determined by measuring the Loop 5′ product (Fig. 3A and data not shown). The decrease in *nifH1* transcript in the BP712 mutant (Fig. 9B), combined with the lack of a processed *nifH1* transcript and the short half-life of the Loop 3′ product in the mutant compared to the long half-life in the same region of the wild-type strain, indicates that the mutation that abolished the promoter for *sava4870.1* also had a major effect on the *nifH1* transcript, probably at the level of transcript processing.

Processing of the *nifD1*, *nifK1*, and *Ava_3931* transcripts. We used 5′ RACE, which can distinguish between processed and primary transcripts (58), to map the 5′ ends of the *nifD1*, *nifK1*, and *Ava_3931* (the conserved gene downstream from *nifK1*) transcripts. In this technique, primary transcripts are treated with TAP, which hydrolyzes the 5′ triphosphate to a monophosphate so that it can be ligated to the RNA linker. However, processed transcripts do not require TAP treatment because they already have a 5′ monophosphate. Using 5′ RACE, with and without TAP treatment, we performed RNA ligase-mediated RT-PCR and then recovered and sequenced the cDNA bands to determine the 5′ ends of the *nifD1*, *nifK1*, and *Ava_3931* transcripts. For all three transcripts, a band was visible from RNA samples that were not treated with TAP (Fig. 10A), indicating that the transcripts are processed from a larger transcript. Despite the diffuse nature of the *nifD1* product, bands for both *nifD1* and *nifK1* were recovered from the gel and were successfully sequenced to identify the 5′ end. While sequence was obtained for the *Ava_3931* product, the sequence at the 5′ end was not of sufficient quality to map the 5′ end, but we estimate that it is close to the start of *Ava_3931*. The locations of these three processing sites predict transcript sizes for *nifH1*, *nifD1*, and *nifK1* (Fig. 10B) that are consistent with the sizes that were first reported in 1986 for the *nifH*, *nifD*, and *nifK* transcripts in *Anabaena* sp. PCC 7120 by Northern blotting (59).

DISCUSSION

NifH plays a crucial role in nitrogenase assembly and function (15, 16, 30, 60). First, it is the enzyme that reduces dinitrogenase. As part of the mature nitrogenase complex, NifH is present in a 2:1 ratio to the NifD and NifK subunits. However, NifH also has a major role in the assembly of nitrogenase, specifically in the maturation of the P cluster and in the maturation and insertion of the M cluster ($MoFe_7S_9C$-homocitrate) into nitrogenase (16). Thus, it

is not surprising that NifH is the most abundant nitrogenase protein. In other diazotrophic bacteria, *nifH* is the first gene on a larger transcript that includes *nifD* and *nifK*, so it was assumed that *nifHDK* in cyanobacteria also comprised an operon under the control of a strong promoter upstream of *nifH* (61, 62). However, as we have shown previously, *nifH1* in *A. variabilis* is driven primarily by the distant *nifB1* promoter, supplemented by a weak promoter in *nifU1* (39). The abundance of the *nifH1* transcript compared to *nifB1*, *nifS1*, and *nifU1* cannot be attributed to the strength of the promoter but does correlate well with the stability of the *nifH1* transcript, which is made by RNA processing at a site 123 bp upstream from the *nifH1* start site. Although the sequences of the intergenic *nifU-nifH* regions of many heterocystous cyanobacteria are not well conserved and do not align well, manual alignment revealed conserved regions that produce a predicted stem-loop structure at the 5′ end of the *nifH1* transcript that is very well conserved (see Fig. S1 in the supplemental material). Stem-loops stabilize transcripts when they are at the extreme 5′ end of the transcript (63). The stabilization of the 5′ end of the transcript when it is double stranded results from the mRNA not being recognized by 5′ exonucleases. According to Emory et al. (63), up to 2 unpaired nucleotides at the 5′ end of a transcript can be tolerated, while 5 or more unpaired nucleotides at the 5′ end of the transcript prevent a stem-loop from having any stabilizing effect. We analyzed mutations in the predicted stem-loop at the 5′ end of *nifH1* to determine the relative importance of the sequence in this region versus the stem-loop structure for *nifH1* transcript abundance. Based on several mutants, it appears that both the sequence and the structure contribute to the abundance of the *nifH1* transcript, and loss of both reduces the amount of transcript by about 90%. Mutant BP706, which completely lacks the first stem-loop structure, had very little *nifH1* mRNA and had slow growth under diazotrophic conditions. The JU423 mutation also had a very deleterious effect on mRNA abundance, probably because the first predicted stem-loop is not very stable ($\Delta G = -9$ versus -21 for FD) and it has several mispaired bases, while the predicted stem-loop in the wild-type strain has only a single mispaired base. The decreased stability of the mutant stem-loop in JU423 increases the probability of a single-stranded target that is recognized for mRNA degradation. The altered stability of the stem-loop in JU423 not only led to a large decrease in transcript levels for *nifH1* but also changed the processing site, which was shifted 8 nucleotides upstream compared to the wild-type strain. This suggests that the altered stem-loop structure in the mutant affected the cleavage site that yields the normal 5′-processed *nifH1* transcript.

In the BP706 mutant, which completely lacks the first stem-loop structure, there was much less *nifH1* transcript than in the wild-type strain, because the *nifH1* transcript was more unstable, and the mutation had a polar effect, resulting in loss of the downstream *nifK1* transcript (Fig. 5A), while the half-life of *nifK1* in the mutant remained nearly the same as in the wild-type strain. While these results may seem contradictory, the quantity of a transcript may decrease while the half-life of the remaining transcript remains the same. Northern blot analysis in *Anabaena* sp. PCC 7120 identified *nifH*, *nifHD*, and *nifHDK* transcripts but not a *nifB-SUHDK* transcript (59). This suggests that the processing event between the *nifU1* and *nifH1* transcripts in *A. variabilis* occurs more rapidly than the processing events within the *nifHDK1* transcript. The *nifK1* transcript has its own processing site (Fig. 10) that likely affects the half-life of the *nifK1* transcript; however, the quantity of *nifK1* transcript is sensitive to the stability of the upstream *nifH1* transcript, because a destabilized *nifHDK1* transcript reduces the abundance of all three individual transcripts. The half-life of the *nifK1* transcript after it is processed from the *nifHDK1* transcript should not be affected by the mutation in the *nifH1* stem-loop structure, which we observed (Table 3). Hence the abundance of the *nifK1* transcript is affected more than the half-life in the stem-loop mutants.

While the abundance of the *nifH1* transcript was expected, it was surprising that, despite large reductions in the amount of *nifH1* transcript in some mutants, there was much less effect on nitrogenase activity. The normal pattern of nitrogenase expression, with a strong peak at about 24 h after nitrogen step down followed by a rapid decline in activity, which remains relatively low (64), suggests that the cells initially make more transcript/enzyme than is required, modulating the amount as the cells become nitrogen replete and store fixed nitrogen in cyanophycin (65). Hence, they may make more enzyme than is required initially to replenish nitrogen reserves and then repress expression, while the mutants may continue to express nitrogenase much longer, which may explain the lack of a major defect in growth of some of the mutants under diazotrophic growth conditions.

Analysis of transcripts in the *nifU1-nifH1* intergenic region revealed a small antisense transcript that began just upstream from the transcriptional processing site for *nifH1* (but is transcribed in the opposite direction). This transcript is evident in the RNA-seq data for *Anabaena* sp. PCC 7120 (42), and its 5′ end was mapped in a global search for primary transcription start sites in the strain (43); however, neither its size nor its function has been described. It appears to be about 200 bp, extending well into the *nifU1* gene, and is upregulated +N compared to transcripts upstream of the *sava4870.1* promoter, though still present in very small amounts. While the amount of antisense transcript increases under −N conditions, that seems to be the result of increased expression of antisense RNA throughout the region, since there is also increased antisense RNA upstream of the *sava4870.1* promoter. Compared to the upstream region, *sava4870.1* RNA is more highly expressed +N than −N, and a mutation in the promoter for *sava4870.1* affected expression only +N, not −N. A mutant lacking the promoter region for *sava4870.1* showed greatly reduced *nifH1* expression, suggesting that the antisense RNA is required for high-level expression of *nifH1*. Although it is possible that the antisense *sava4870.1* RNA that is already present in heterocysts helps to stabilize the *nifH1* transcript, leading to a decrease in *nifH1* transcript in the mutant, this seems unlikely, because the mutant and wild-type strains show nearly identical levels of *sava4870.1* antisense RNA under nitrogen-deficient growth conditions (Fig. 9A). More likely, the effect of the mutation may not be directly related to loss of the *sava4870.1* antisense RNA. The *sava4870.1* promoter mutation is very close to the processing site for the *nifH1* transcript and did abolish processing of the *nifH1* transcript. Further, a mutant with a 38-bp deletion that began 4-bp downstream from the end of *nifU1*, and thus was within the *sava4870.1* gene, had no phenotype (data not shown), supporting the hypothesis that *sava4870.1* is not directly involved in *nifH1* expression. We also observed that there was a 50- to 100-fold increase in expression of *nifH1* antisense transcripts in cells grown in the absence of fixed nitrogen compared to cells grown with fixed nitrogen. While the amount of antisense tran-

script compared to sense for *nifH1* is very low (about 2.5% as much), it is difficult to imagine the role of this antisense transcript in the expression of nitrogenase genes.

In *Anabaena* sp. PCC 7120, the transcripts for *nifHDK*, as determined by Northern blots, suggested that they all derived from a single transcript initiated upstream of *nifH*. The *nifH* probe hybridized to transcripts of about 4.7 kb, 2.8 kb, and 1.1 kb; *nifD* hybridized to transcripts of 4.7 kb and 2.8 kb, and *nifK* hybridized to the 4.7-kb transcript (59). These sizes correspond to transcript junctions between *nifH* and *nifD* and between *nifD* and *nifK*. If the *nifB* promoter is the primary promoter for transcription of the entire *nif* cluster, then it seems unlikely that termination of transcription at these junctions is the only mechanism of transcript regulation, although it could play a role, since the amount of transcript for genes downstream of *nifK1* is much less than for *nifK1* itself (46). However, we determined that the transcript made from the *nifB1* and internal *nifU1* promoters is processed just upstream of *nifD1*, *nifK1*, and *Ava_3931* (Fig. 10), resulting in predicted transcript sizes that are consistent with the reported sizes for the *nifH*, *nifD*, and *nifK1* transcripts in *Anabaena* sp. PCC 7120 (59). However, the presence of a strong 2.8-kb band that hybridizes to *nifH* and *nifD* in *Anabaena* sp. PCC 7120 (59) suggests that processing between *nifH* and *nifD* is not efficient. The region around the 5′ end of *nifD1* has no strong predicted secondary structure; however, the 5′ end of *nifK1* is within a strong predicted single stem-loop structure ($\Delta G = -31.7$). The sizes and abundances of the *nifD1* and *nifK1* transcripts in *A. variabilis* may reflect a combination of termination of transcription, transcriptional processing, and transcript stability; however, the relative amounts of *nifH1*, *nifD1*, and *nifK1* transcripts normalized to *nifB1* are roughly proportional to their half-lives (Table 3), suggesting that stability is very important in maintaining the stoichiometry of the three transcripts. The 7-fold decrease in the amount of *nifE1* transcript compared to *nifK1* (46), however, suggests that this large drop may result from both transcriptional termination downstream of *nifK1* and the much shorter half-life of *nifE1* than of *nifK1* (Table 3). Despite multiple attempts, we have not been successful in finding the 5′ end of *nifE1* by 5′ RACE.

The data presented here support the conclusion that expression of the *nifH1*, *nifD1*, and *nifK1* genes, encoding the nitrogenase proteins that are required in the greatest abundance for nitrogen fixation, depends on transcript processing. Further, the stability of the *nifH1*, *nifD1*, and *nifK1* transcripts correlates with the amount of transcript (46), and at least for *nifH1*, sequences near the transcriptional processing site are important in processing and transcript stability. The predicted secondary structures in the intergenic regions of *nifU1-nifH1* and *nifD1-nifK1* may play a role in the regulation of the transcript abundances of *nifH1* and *nifK1*; however, at least in the case of *nifH1*, the sequences around the processing site appear to be equally important for transcript stability.

ACKNOWLEDGMENT

Support for this research was provided by National Science Foundation grant MCB-1052241.

REFERENCES

1. **Kumar K, Mella-Herrera RA, Golden JW.** 2010. Cyanobacterial heterocysts. Cold Spring Harbor Perspect Biol **2:**a000315. http://dx.doi.org/10.1101/cshperspect.a000315.
2. **Herrero A, Picossi S, Flores E.** 2013. Gene expression during heterocyst differentiation, p 281–329. *In* Franck C, Corinne C-C (ed), Advances in botanical research, vol 65. Academic Press, Waltham, MA.
3. **Muro-Pastor AM, Hess WR.** 2012. Heterocyst differentiation: from single mutants to global approaches. Trends Microbiol **20:**548–557. http://dx.doi.org/10.1016/j.tim.2012.07.005.
4. **Murry MA, Wolk CP.** 1989. Evidence that the barrier to the penetration of oxygen into heterocysts depends upon two layers of the cell envelope. Arch Microbiol **151:**469–474. http://dx.doi.org/10.1007/BF00454860.
5. **Walsby AE.** 2007. Cyanobacterial heterocysts: terminal pores proposed as sites of gas exchange. Trends Microbiol **15:**340–349. http://dx.doi.org/10.1016/j.tim.2007.06.007.
6. **Valladares A, Herrero A, Pils D, Schmetterer G, Flores E.** 2003. Cytochrome c oxidase genes required for nitrogenase activity and diazotrophic growth in *Anabaena* sp PCC 7120. Mol Microbiol **47:**1239–1249. http://dx.doi.org/10.1046/j.1365-2958.2003.03372.x.
7. **Thiel T, Pratte B.** 2014. Regulation of three nitrogenase gene clusters in the cyanobacterium *Anabaena variabilis* ATCC 29413. Life **4:**944–967. http://dx.doi.org/10.3390/life4040944.
8. **Thiel T.** 1993. Characterization of genes for an alternative nitrogenase in the cyanobacterium *Anabaena variabilis*. J Bacteriol **175:**6276–6286.
9. **Thiel T.** 1996. Isolation and characterization of the *vnfEN* genes of the cyanobacterium *Anabaena variabilis*. J Bacteriol **178:**4493–4499.
10. **Thiel T.** 2004. Nitrogen fixation in heterocyst-forming cyanobacteria, p 73–110. *In* Klipp W, Masepohl B, Gallon JR, Newton WE (ed), Genetics and regulation of nitrogen fixing bacteria. Kluwer Academic Publishers, Dordrecht, The Netherlands.
11. **Pratte BS, Eplin K, Thiel T.** 2006. Cross-functionality of nitrogenase components NifH1 and VnfH in *Anabaena variabilis*. J Bacteriol **188:**5806–5811. http://dx.doi.org/10.1128/JB.00618-06.
12. **Thiel T, Pratte B.** 2001. Effect on heterocyst differentiation of nitrogen fixation in vegetative cells of the cyanobacterium *Anabaena variabilis* ATCC 29413. J Bacteriol **183:**280–286. http://dx.doi.org/10.1128/JB.183.1.280-286.2001.
13. **Lancaster KM, Roemelt M, Ettenhuber P, Hu Y, Ribbe MW, Neese F, Bergmann U, DeBeer S.** 2011. X-ray emission spectroscopy evidences a central carbon in the nitrogenase iron-molybdenum cofactor. Science **334:**974–977. http://dx.doi.org/10.1126/science.1206445.
14. **Spatzal T, Aksoyoglu M, Zhang L, Andrade SLA, Schleicher E, Weber S, Rees DC, Einsle O.** 2011. Evidence for interstitial carbon in nitrogenase FeMo cofactor. Science **334:**940. http://dx.doi.org/10.1126/science.1214025.
15. **Rubio LM, Ludden PW.** 2008. Biosynthesis of the iron-molybdenum cofactor of nitrogenase. Annu Rev Microbiol **62:**93–111. http://dx.doi.org/10.1146/annurev.micro.62.081307.162737.
16. **Hu Y, Ribbe MW.** 2013. Biosynthesis of the iron-molybdenum cofactor of nitrogenase. J Biol Chem **288:**13173–13177. http://dx.doi.org/10.1074/jbc.R113.454041.
17. **Lawson DM, Smith BE.** 2002. Molybdenum nitrogenases: a crystallographic and mechanistic view. Met Ions Biol Syst **39:**75–119.
18. **Zheng L, White RH, Cash VL, Jack RF, Dean DR.** 1993. Cysteine desulfurase activity indicates a role for NIFS in metallocluster biosynthesis. Proc Natl Acad Sci U S A **90:**2754–2758. http://dx.doi.org/10.1073/pnas.90.7.2754.
19. **Yuvaniyama P, Agar JN, Cash VL, Johnson MK, Dean DR.** 2000. NifS-directed assembly of a transient [2Fe-2S] cluster within the NifU protein. Proc Natl Acad Sci U S A **97:**599–604. http://dx.doi.org/10.1073/pnas.97.2.599.
20. **Wiig JA, Hu Y, Ribbe MW.** 2011. NifEN-B complex of *Azotobacter vinelandii* is fully functional in nitrogenase FeMo cofactor assembly. Proc Natl Acad Sci U S A **108:**8623–8627. http://dx.doi.org/10.1073/pnas.1102773108.
21. **Curatti L, Hernandez JA, Igarashi RY, Soboh B, Zhao D, Rubio LM.** 2007. In vitro synthesis of the iron molybdenum cofactor of nitrogenase from iron, sulfur, molybdenum, and homocitrate using purified proteins. Proc Natl Acad Sci U S A **104:**17626–17631. http://dx.doi.org/10.1073/pnas.0703050104.
22. **Kaiser JT, Hu Y, Wiig JA, Rees DC, Ribbe MW.** 2011. Structure of precursor-bound NifEN: a nitrogenase FeMo cofactor maturase/insertase. Science **331:**91–94. http://dx.doi.org/10.1126/science.1196954.
23. **Kim S, Burgess BK.** 1996. Evidence for the direct interaction of the nifW gene product with the MoFe protein. J Biol Chem **271:**9764–9770. http://dx.doi.org/10.1074/jbc.271.16.9764.

24. **Hernandez JA, Igarashi RY, Soboh B, Curatti L, Dean DR, Ludden PW, Rubio LM.** 2007. NifX and NifEN exchange NifB cofactor and the VK-cluster, a newly isolated intermediate of the iron-molybdenum cofactor biosynthetic pathway. Mol Microbiol **63:**177–192. http://dx.doi.org/10.1111/j.1365-2958.2006.05514.x.
25. **Hu Y, Fay AW, Dos Santos PC, Naderi F, Ribbe MW.** 2004. Characterization of *Azotobacter vinelandii nifZ* deletion strains Indication of stepwise MoFe protein assembly. J Biol Chem **279:**54963–54971. http://dx.doi.org/10.1074/jbc.M408983200.
26. **Hu Y, Fay AW, Lee CC, Ribbe MW.** 2007. P-cluster maturation on nitrogenase MoFe protein. Proc Natl Acad Sci U S A **104:**10424–10429. http://dx.doi.org/10.1073/pnas.0704297104.
27. **Hernandez JA, Curatti L, Aznar CP, Perova Z, Britt RD, Rubio LM.** 2008. Metal trafficking for nitrogen fixation: NifQ donates molybdenum to NifEN/NifH for the biosynthesis of the nitrogenase FeMo-cofactor. Proc Natl Acad Sci U S A **105:**11679–11684. http://dx.doi.org/10.1073/pnas.0803576105.
28. **Gavini N, Tungtur S, Pulakat L.** 2006. Peptidyl-prolyl cis/trans isomerase-independent functional *nifH* mutant of *Azotobacter vinelandii*. J Bacteriol **188:**6020–6025. http://dx.doi.org/10.1128/JB.00379-06.
29. **Howard KS, McLean PA, Hansen FB, Lemley PV, Koblan KS, Orme-Johnson WH.** 1986. *Klebsiella pneumoniae nifM* gene product is required for stabilization and activation of nitrogenase iron protein in *Escherichia coli*. J Biol Chem **261:**772–778.
30. **Rubio LM, Ludden PW.** 2005. Maturation of nitrogenase: a biochemical puzzle. J Bacteriol **187:**405–414. http://dx.doi.org/10.1128/JB.187.2.405-414.2005.
31. **Rubio LM, Singer SW, Ludden PW.** 2004. Purification and characterization of NafY (apodinitrogenase gamma subunit) from Azotobacter vinelandii. J Biol Chem **279:**19739–19746. http://dx.doi.org/10.1074/jbc.M400965200.
32. **Pratte BS, Thiel T.** 2006. High-affinity vanadate transport system in the cyanobacterium *Anabaena variabilis* ATCC 29413. J Bacteriol **188:**464–468. http://dx.doi.org/10.1128/JB.188.2.464-468.2006.
33. **Thiel T, Pratte B.** 2013. Alternative nitrogenases in *Anabaena variabilis*: the role of molybdate and vanadate in nitrogenase gene expression and activity. Adv Microbiol **3:**87–95. http://dx.doi.org/10.4236/aim.2013.36A011.
34. **Martinez-Argudo I, Little R, Shearer N, Johnson P, Dixon R.** 2005. Nitrogen fixation: key genetic regulatory mechanisms. Biochem Soc Trans **33:**152–156. http://dx.doi.org/10.1042/BST0330152.
35. **Mella-Herrera RA, Neunuebel MR, Kumar K, Saha SK, Golden JW.** 2011. The *sigE* gene is required for normal expression of heterocyst-specific genes in *Anabaena* sp. strain PCC 7120. J Bacteriol **193:**1823–1832. http://dx.doi.org/10.1128/JB.01472-10.
36. **Valladares A, Muro-Pastor AM, Fillat MF, Herrero A, Flores E.** 1999. Constitutive and nitrogen-regulated promoters of the *petH* gene encoding ferredoxin:NADP+ reductase in the heterocyst-forming cyanobacterium *Anabaena* sp. FEBS Lett **449:**159–164. http://dx.doi.org/10.1016/S0014-5793(99)00404-4.
37. **Ramasubramanian TS, Wei TF, Golden JW.** 1994. Two *Anabaena* sp. strain PCC 7120 DNA-binding factors interact with vegetative cell- and heterocyst-specific genes. J Bacteriol **176:**1214–1223.
38. **Picossi S, Flores E, Herrero A.** 2014. ChIP analysis unravels an exceptionally wide distribution of DNA binding sites for the NtcA transcription factor in a heterocyst-forming cyanobacterium. BMC Genomics **15:**22. http://dx.doi.org/10.1186/1471-2164-15-22.
39. **Ungerer JL, Pratte BS, Thiel T.** 2010. RNA processing of nitrogenase transcripts in the cyanobacterium *Anabaena variabilis*. J Bacteriol **192:**3311–3320. http://dx.doi.org/10.1128/JB.00278-10.
40. **Mulligan ME, Haselkorn R.** 1989. Nitrogen fixation (*nif*) genes of the cyanobacterium *Anabaena* species strain PCC 7120. The *nifB-fdxN-nifS-nifU* operon. J Biol Chem **264:**19200–19207.
41. **Jackman DM, Mulligan ME.** 1995. Characterization of a nitrogen-fixation (*nif*) gene cluster from *Anabaena azollae* 1a shows that closely related cyanobacteria have highly variable but structured intergenic regions. Microbiology **141:**2235–2244. http://dx.doi.org/10.1099/13500872-141-9-2235.
42. **Flaherty BL, Van Nieuwerburgh F, Head SR, Golden JW.** 2011. Directional RNA deep sequencing sheds new light on the transcriptional response of *Anabaena* sp. strain PCC 7120 to combined-nitrogen deprivation. BMC Genomics **12:**332. http://dx.doi.org/10.1186/1471-2164-12-332.
43. **Mitschke J, Vioque A, Haas F, Hess WR, Muro-Pastor AM.** 2011. Dynamics of transcriptional start site selection during nitrogen stress-induced cell differentiation in *Anabaena* sp. PCC7120. Proc Natl Acad Sci U S A **108:**20130–20135. http://dx.doi.org/10.1073/pnas.1112724108.
44. **Borthakur D, Basche M, Buikema WJ, Borthakur PB, Haselkorn R.** 1990. Expression, nucleotide sequence and mutational analysis of two open reading frames in the *nif* gene region of *Anabaena* sp. strain PCC7120. Mol Gen Genet **221:**227–234.
45. **Böhme H, Haselkorn R.** 1988. Molecular cloning and nucleotide sequence analysis of the gene coding for heterocyst ferredoxin from the cyanobacterium *Anabaena* sp. strain PCC 7120. Mol Gen Genet **214:**278–285. http://dx.doi.org/10.1007/BF00337722.
46. **Pratte BS, Thiel T.** 2014. Regulation of nitrogenase gene expression by transcript stability in the cyanobacterium *Anabaena variabilis*. J Bacteriol **196:**3609–3621. http://dx.doi.org/10.1128/JB.02045-14.
47. **Pratte BS, Sheridan R, James JA, Thiel T.** 2013. Regulation of V-nitrogenase genes in *Anabaena variabilis* by RNA processing and by dual repressors. Mol Microbiol **88:**413–424. http://dx.doi.org/10.1111/mmi.12197.
48. **Allen MB, Arnon DI.** 1955. Studies on nitrogen-fixing blue-green algae. I. Growth and nitrogen fixation by *Anabaena cylindrica* Lemm. Plant Physiol **30:**366–372.
49. **Black TA, Cai Y, Wolk CP.** 1993. Spatial expression and autoregulation of *hetR*, a gene involved in the control of heterocyst development in *Anabaena*. Mol Microbiol **9:**77–84. http://dx.doi.org/10.1111/j.1365-2958.1993.tb01670.x.
50. **Elhai J, Wolk CP.** 1988. Conjugal transfer of DNA to cyanobacteria. Methods Enzymol **167:**747–754. http://dx.doi.org/10.1016/0076-6879(88)67086-8.
51. **Cai Y, Wolk CP.** 1990. Use of a conditionally lethal gene in *Anabaena* sp. strain PCC 7120 to select for double recombinants and to entrap insertion sequences. J Bacteriol **172:**3138–3145.
52. **Ungerer JL, Pratte BS, Thiel T.** 2008. Regulation of fructose transport and its effect on fructose toxicity in *Anabaena* spp. J Bacteriol **190:**8115–8125. http://dx.doi.org/10.1128/JB.00886-08.
53. **Thiel T, Wolk CP.** 1987. Conjugal transfer of plasmids to cyanobacteria. Methods Enzymol **153:**232–243. http://dx.doi.org/10.1016/0076-6879(87)53056-7.
54. **Miller J.** 1972. Experiments in molecular genetics, p 352–355. Cold Spring Harbor Laboratory Press, Cold Spring Harbor, NY.
55. **Chen Y, Indurthi DC, Jones SW, Papoutsakis ET.** 2011. Small RNAs in the genus *Clostridium*. mBio **2:**e00340-10. http://dx.doi.org/10.1128/mBio.00340-10.
56. **Chenna R, Sugawara H, Koike T, Lopez R, Gibson TJ, Higgins DG, Thompson JD.** 2003. Multiple sequence alignment with the Clustal series of programs. Nucleic Acids Res **31:**3497–3500. http://dx.doi.org/10.1093/nar/gkg500.
57. **Zuker M.** 2003. Mfold Web server for Nucleic acid folding and hybridization prediction. Nucleic Acids Res **31:**3406–3415. http://dx.doi.org/10.1093/nar/gkg595.
58. **Bensing BA, Meyer BJ, Dunny GM.** 1996. Sensitive detection of bacterial transcription initiation sites and differentiation from RNA processing sites in the pheromone-induced plasmid transfer system of *Enterococcus faecalis*. Proc Natl Acad Sci U S A **93:**7794–7799. http://dx.doi.org/10.1073/pnas.93.15.7794.
59. **Haselkorn R, Golden JW, Lammers PJ, Mulligan ME.** 1986. Developmental rearrangement of cyanobacterial nitrogen-fixation genes. Trends Genet **2:**255–259. http://dx.doi.org/10.1016/0168-9525(86)90258-1.
60. **Hu Y, Ribbe MW.** 2011. Biosynthesis of the metalloclusters of molybdenum nitrogenase. Microbiol Mol Biol Rev **75:**664–677. http://dx.doi.org/10.1128/MMBR.05008-11.
61. **Lammers PJ, Haselkorn R.** 1983. Sequence of the nifD gene coding for the a subunit of dinitrogenase from the cyanobacterium Anabaena. Proc Natl Acad Sci U S A **80:**4723–4727. http://dx.doi.org/10.1073/pnas.80.15.4723.
62. **Mevarech M, Rice D, Haselkorn R.** 1980. Nucleotide sequence of a cyanobacterial nifH gene coding for nitrogenase reductase. Proc Natl Acad Sci U S A **77:**6476–6480. http://dx.doi.org/10.1073/pnas.77.11.6476.
63. **Emory SA, Bouvet P, Belasco JG.** 1992. A 5′-terminal stem-loop structure can stabilize mRNA in *Escherichia coli*. Genes Dev **6:**135–148. http://dx.doi.org/10.1101/gad.6.1.135.
64. **Schutz K, Happe T, Troshina O, Lindblad P, Leitao E, Oliveira P, Tamagnini P.** 2004. Cyanobacterial H_2 production—a comparative analysis. Planta **218:**350–359. http://dx.doi.org/10.1007/s00425-003-1113-5.
65. **Burnat M, Herrero A, Flores E.** 2014. Compartmentalized cyanophycin metabolism in the diazotrophic filaments of a heterocyst-forming cyano-

bacterium. Proc Natl Acad Sci U S A **111:**3823–3828. http://dx.doi.org/10.1073/pnas.1318564111.
66. **Currier TC, Wolk CP.** 1979. Characteristics of *Anabaena variabilis* influencing plaque formation by cyanophage N-1. J Bacteriol **139:**88–92.
67. **Herrero A, Wolk CP.** 1986. Genetic mapping of the chromosome of the cyanobacterium, *Anabaena variabilis*. Proximity of the structural genes for nitrogenase and ribulose bisphosphate carboxylase. J Biol Chem **261:** 7748–7754.
68. **Vieira J, Messing J.** 1982. The pUC plasmids, an M13mp7-derived system for insertion mutagenesis and sequencing with synthetic universal primers. Gene **19:**259–268. http://dx.doi.org/10.1016/0378-1119(82)90015-4.
69. **Markowitz VM, Chen I-MA, Palaniappan K, Chu K, Szeto E, Grechkin Y, Ratner A, Jacob B, Huang J, Williams P, Huntemann M, Anderson I, Mavromatis K, Ivanova NN, Kyrpides NC.** 2012. IMG: the integrated microbial genomes database and comparative analysis system. Nucleic Acids Res **40:**D115–D122. http://dx.doi.org/10.1093/nar/gkr1044.